A Systematic Design of A Dual-loop PID Controller for An Inverted Pendulum on A Moving Cart

Shiang Cao[1], Sachin Giri[2], Kenneth Furrer[1], and YangQuan Chen[1†]

***Abstract*—The inverted pendulum on a cart is a classical benchmark for control design and is frequently used as an introduction to multivariable systems in laboratory settings. While it is often assumed that state-space methods are necessary to simultaneously regulate cart position and pendulum angle, this paper demonstrates that a classical control approach is not only feasible but also offer advantages in certain cases. First, the fundamental limitations of controller design based on a single measurement are examined, highlighting the necessity of directly measuring the pendulum's rotation angle. The problem is then reformulated using two cascaded transfer functions, which provide the key insight required for effective control. A minor loop is introduced to stabilize the pendulum, while a main loop regulates the cart position, thereby achieving greater separation of the dynamics and improved overall performance.**

***Index Terms*—Inverted pendulum, Nonminimum-phase, PID control**

I. Background and Introduction

The inverted pendulum is one of the most classical benchmark problems in control engineering. Although it is widely used in undergraduate courses to illustrate fundamental control concepts, its nonlinearity and inherent instability make stabilization and regulation challenging. In addition, the system is underactuated, which further increases the difficulty of controller design [1].

Numerous strategies have been applied to the inverted pendulum problem. State-space methods such as pole placement, linear quadratic regulation (LQR), and model predictive control (MPC) have been widely employed to stabilize both the pendulum angle and the cart position simultaneously [2]. In addition, fuzzy logic controllers have also been explored for this problem [3]. The proportional–integral–derivative (PID) controller, owing to its simplicity and widespread industrial adoption, has likewise been studied for the stabilization of the inverted pendulum on a cart. In typical designs, two PID controllers are used to regulate the pendulum angle and the cart position separately [4]. However, such controllers are often designed through a trial-and-error process [1], [2], [4], which makes parameter tuning inefficient and performance difficult to guarantee. To address this issue, this paper presents a systematic approach to PID controller design by reformulating the inverted pendulum system into a series configuration. The proposed structure employs an inner loop to stabilize the pendulum dynamics and an outer loop to regulate the cart position, thereby achieving a clearer separation of the dynamics. Therefore, the controller parameters are determined based on frequency-response criteria, which avoids trial-and-error tuning and provides a more systematic design process.

[1] Department of Mechanical Engineering & Aerospace, University of California Merced, [2] Electrical Engineering and Computer Science Graduate Group, University of California, Merced, CA, USA, [†] Corresponding author, (scao32, sachingiri, kfurrer, ychen53)@ucmerced.edu

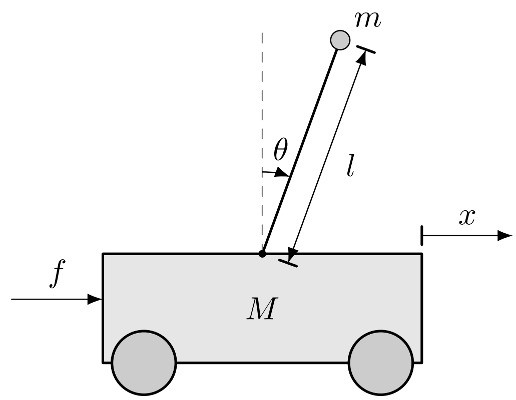

Fig. 1: A schematic representation of an inverted pendulum on a cart.

II. System Model

A schematic representation of an inverted pendulum on a cart is shown in Figure 1. The input to this system is a linear force on the cart. The outputs of the system are the cart position x and pendulum angle θ. The nonlinear system model of the inverted pendulum on a cart is derived as [5]:

$$\begin{aligned}\ddot{x} &= \frac{1}{\lambda+\sin^2\theta(t)}\left[\frac{f(t)}{m}+\dot{\theta}^2(t)l\sin\theta(t)-g\cos\theta(t)\sin\theta(t)\right],\\ \ddot{\theta} &= \frac{1}{l\lambda+\sin^2\theta(t)}\Bigg[-\frac{f(t)}{m}\cos\theta(t)+\dot{\theta}^2(t)l\sin\theta(t)\cos\theta(t)\\ &\quad+(1+\lambda)g\sin\theta(t)\Bigg],\end{aligned} \tag{1}$$

where $\lambda = M/m$. The equation set shown in (1) can be linearized given the common small angle assumptions of

$$\begin{aligned}&\cos\theta \approx 1,\\ &\sin\theta \approx \theta,\\ &\dot{\theta} \ll 1 \implies \dot{\theta}^2 = 0.\end{aligned}$$

The resulting linear equations are

$$\begin{aligned}\ddot{x} &= \frac{1}{\lambda}\left[\frac{f}{m}-g\theta\right],\\ \ddot{\theta} &= \frac{1}{l\lambda}\left[-\frac{f}{m}+(1+\lambda)g\theta\right].\end{aligned} \tag{2}$$

By applying the Laplace transform, the transfer function from f to x is derived as

$$G_1 = \frac{\mathcal{X}}{\mathcal{F}} = \frac{1}{M}\frac{s^2 - a^2}{s^2(s^2 - b^2)}, \tag{3}$$

where $a^2 = \frac{g}{l}$, and $b^2 = \frac{1+\lambda}{\lambda}a^2$. It is evident from this expression that the system is open-loop unstable and contains a non-minimum-phase zero.

III. Fundamental Limitations for SISO Control

This section examines the inherent limitations of controller design when only the cart position x is measured. Let $z = a$ and $p = b$ denote the right-half-plane (RHP) zero and pole, respectively. Since $z < p$, it follows from [6] that the plant cannot be stabilized by any stable controller. In addition, for any stable feedback system as shown in Fig. 2, the undershoot of the step response x_{us} must satisfy the bound [7]:

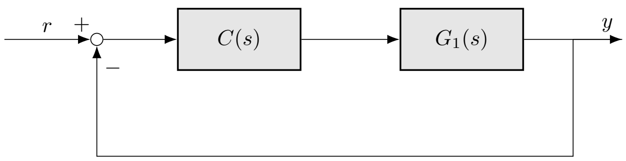

Fig. 2: A block diagram of the feedback control.

$$x_{us} \geq \frac{z}{p - z}. \tag{4}$$

For example, let $M = m = 0.5, l = 1$, and $g = 10$. The RHP pole and zero are $p = \sqrt{20}$, and $z = \sqrt{10}$, respectively. According to (4), the undershoot bound is $x_{us} \geq 2.41$. Using the polynomial approach [5], several controllers are designed to place the closed-loop poles in the stable region. The step responses of these systems are shown in Fig. 3, where it can be observed that all undershoots exceed the theoretical bound. From the frequency-domain perspective, the presence of the RHP pole and zero also imposes limitations on controller design. Let S denote the sensitivity function of the feedback system shown in Fig. 2:

$$S(s) = \frac{1}{1 + G(s)C(s)}.$$

The Bode sensitivity integral also imposes a fundamental constraint on the sensitivity function S [8]:

$$\int_0^\infty \ln\left|S(j\omega)\right|, d\omega = \pi \sum \Re(p_i), \tag{5}$$

where p_i are the open-loop RHP poles. This relation implies that open-loop unstable poles inevitably result in a net loss of disturbance attenuation across the frequency spectrum. Furthermore, the sensitivity peak for this feedback system is also bounded by [9]:

$$\|S\|_\infty \geq \frac{|z + p|}{|z - p|}. \tag{6}$$

This inequality indicates that the control performance will deteriorate significantly if the right-half-plane (RHP) pole and zero are not sufficiently separated.

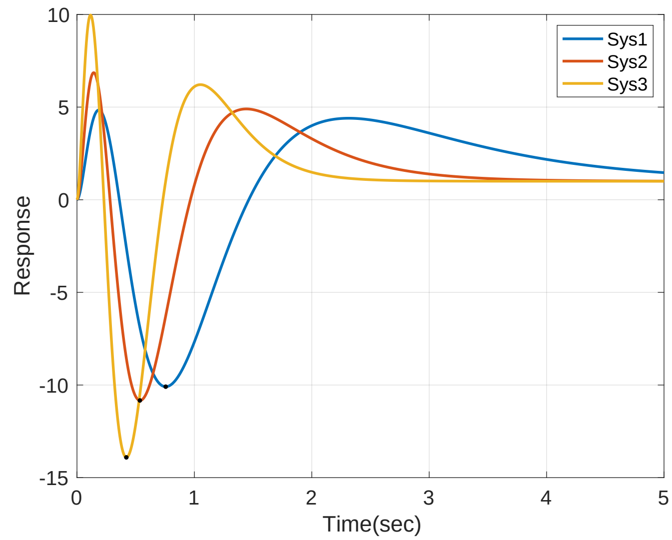

Fig. 3: Step responses of the feedback system under different controllers. In every case, the undershoot exceeds the theoretical lower bound of $x_{us} \geq 2.41$, confirming the validity of the limitation.

IV. A Dual PID controller

This section presents the design of a controller that utilizes both the cart position x and the pendulum angle θ as feedback measurements. The transfer function from f to θ is

$$G_2(s) = \frac{\Theta}{\mathcal{F}} = \frac{-1}{Ml(s^2 - b^2)}. \tag{7}$$

Accordingly, the system can be represented in a parallel structure, where the input is the applied force and the outputs are the pendulum angle and cart position. The corresponding block diagram representation is shown in Fig. 4. Using elementary block diagram transformations, the parallel form of Fig. 4 can be transformed into a series arrangement as shown in Fig. 5. The first function in the series transfers force $\mathcal{F}$ into pendulum angle Θ, described by the transfer function G_2. The second

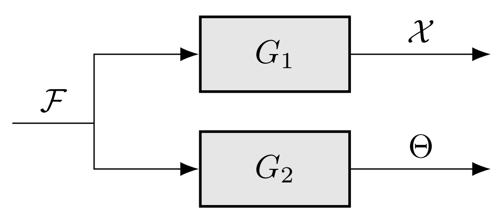

Fig. 4: A block diagram of the parallel transfer function structure.

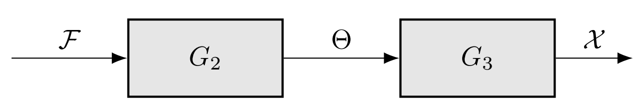

Fig. 5: A block diagram of the series transfer function structure.

function transfers angle Θ into cart position $\mathcal{X}$, and is denoted by G_3. It is clear that

$$G_3 = \frac{G_1}{G_2} = \frac{-l(s^2 - a^2)}{s^2}. \tag{8}$$

The strength of the series arrangement is that it admits an inner, or so-called minor, loop feedback structure as part of a possible control scheme. Minor loop feedback is a powerful concept that uses feedback to control a troublesome series element thus reducing its effects on the outer, or major, loop [10].

The controller design problem centers around creating an independent, stable inner loop around the pendulum. After a controller is created that stabilizes the inner loop, the design is completed by creating a second stable outer loop. To stabilize the inner loop, a PD controller is introduced.

$$C_i = k_i(s + d_i). \tag{9}$$

The closed-loop characteristic equation becomes:

$$Ml(s^2 - b^2) - k_i(s + d_i) = 0.$$

Stability requires the gain and zero to satisfy

$$k_i < 0, \quad d_i > 0, \text{and } k_i d_i < -Mlb^2.$$

When designing the controller, the closed-loop transfer function of the inner pendulum loop must naturally be considered. However, once stabilized, the inner loop presents no particular difficulties, and a variety of cart position controllers may be implemented. For example, suppose k_i and d_i are chosen such that both closed-loop poles are real and lie in the left half-plane. The resulting inner-loop transfer function is

$$G_{2CL} = \frac{k_1(s + d_1)}{(s + p_1)(s + p_2)}, \tag{10}$$

where $p_1, p_2 \in \mathbb{R}$, and $p_1 \geq p_2 > 0$ denote the real closed-loop poles. The dominant pole of the subsystem is now at p_2. In general, the pendulum subsystem bandwidth should be higher than the cart bandwidth thus implying more rapid correction of pendulum errors and slower correction of cart errors. Separation of component bandwidths is one of the strengths of the transfer function method [11].

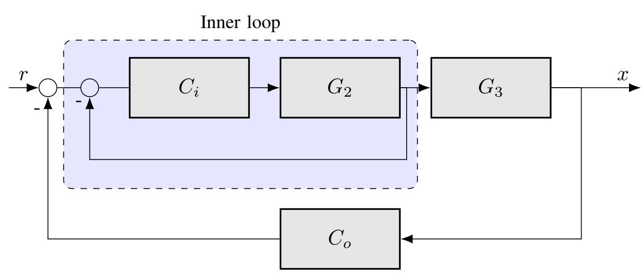

Fig. 6: The feedback structure of the series system.

The combined open loop transfer function of the stabilized pendulum and the series cart transfer function can be expressed as:

$$G = \frac{-k_1 l(s + d_1)(s - a)(s + a)}{s^2(s + p_1)(s + p_2)}. \tag{11}$$

To further stabilize the combined system under specified frequency-domain criteria, an additional controller can be introduced. The overall control structure is illustrated in Fig. 6.

As an illustrative example, consider the parameter values $M = m = 0.5, l = 1, a^2 = 10, b^2 = 20$ and $g = 10$. Selecting controller gains $k_i = -4$, and $d_i = 4.375$, the open-loop function of the combined system is

$$G = \frac{-8(s + 4.375)(s - \sqrt{10})(s + \sqrt{10})}{s^2(s + 5)(s + 3)}. \tag{12}$$

The crossover frequency is selected to satisfy

$$w_c < \min(p_2, a)$$

In this example, the design specifications are set to a crossover frequency of $\omega_c = 1$ rad/s and a desired phase margin of $\phi = 60°$. To meet these criteria, a second PD controller is introduced, defined as:

$$C_o = k_o(s + d_o). \tag{13}$$

At the chosen crossover frequency, the open-loop magnitude and phase of G are evaluated as

$$|G(j\omega_c)| = 24.49, \quad \angle G(j\omega_c) = -193°.$$

To achieve the desired phase margin at ω_c, the parameter d_o is selected according to

$$\frac{\omega_c}{d_o} = \tan\left[\phi - (180° + \angle(G(j\omega_c)))\right], \tag{14}$$

while the gain k_o is chosen as:

$$k_o = \frac{1}{|G(j\omega_c)|}. \tag{15}$$

The resulting loop transfer function exhibits the frequency response shown in the Bode plot in Fig. 7. The plot confirms

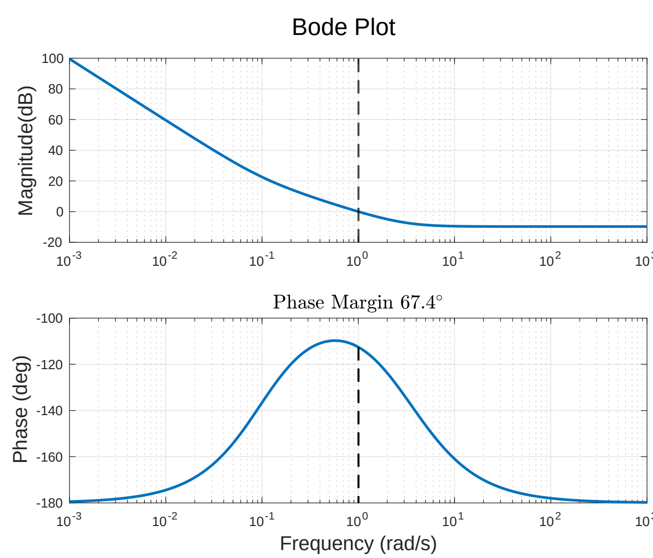

Fig. 7: Bode plot of the loop function

that the controller design achieves the specified crossover frequency and ensures the desired phase margin.

A. Simulation results and discussion

For simulation and implementation, the PD controller is expressed in the practical form:

$$C_o(s) = k_o \left(d_0 + \frac{Ns}{s+N} \right), \tag{16}$$

with $N = 20\omega_c$. Based on the frequency-domain specifications, the controller coefficients are recalculated accordingly. The closed-loop step response under measurement noise is illustrated in Fig. 8. Compared with the results shown in Fig. 3, there is a substantial improvement in the time response. Furthermore, the lower bound on undershoot imposed by (4) is surpassed, demonstrating that smaller undershoot values can be achieved.

In addition, the influence of model uncertainty is analyzed in this section. Two key factors are taken into account: the mass ratio, $\lambda = \frac{M}{m}$, and the pendulum length, l. First, the mass ratio is varied from 0.5 to 1.5, and the corresponding envelope of the step responses is shown in Fig. 9. Interestingly, according to (6), when only the position measurement is used for feedback, reducing the mass ratio λ increases the peak of the sensitivity function, which typically indicates degraded performance. In contrast, under the proposed dual PID scheme, as shown in Fig. 9, reducing λ does not produce a significant adverse effect on the response. These results highlight the importance of sensor placement for control performance and demonstrate the necessity of measuring the pendulum's rotation angle. Furthermore, the pendulum length is varied from 0.1 to 1.9, as illustrated in Fig.10. The results indicate that position control is relatively insensitive to changes in pendulum length, whereas a reduction in length may introduce difficulties in stabilizing the pendulum.

V. Conclusion and Future Work

The study highlights the fundamental limitations of SISO control based solely on position measurement, where right-half-plane poles and zeros impose strict performance bounds.

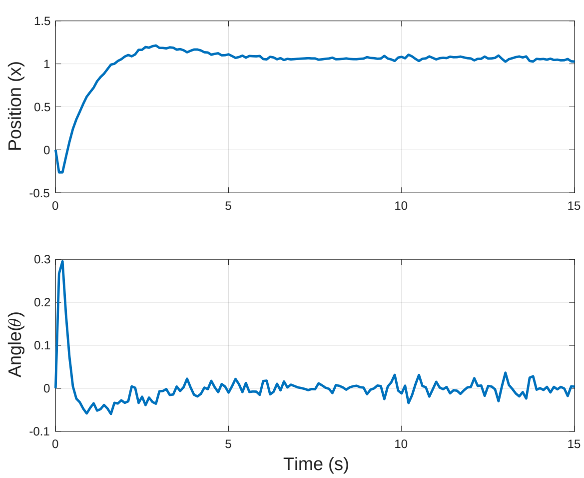

Fig. 8: Step response of the feedback system under measurement noise.

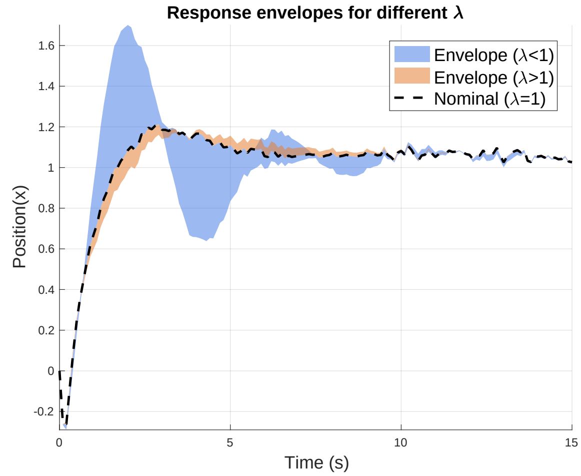

(a) Envelop of the position response λ

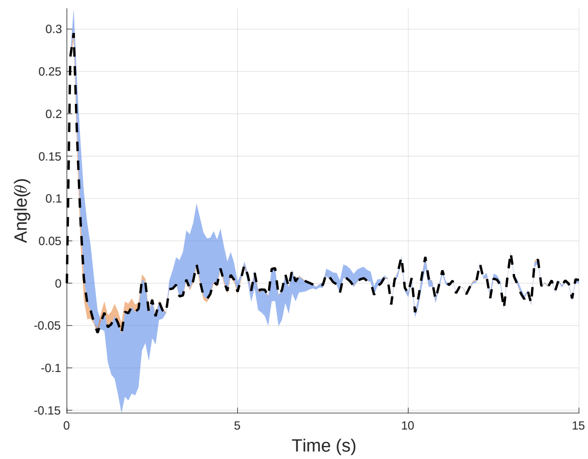

(b) Envelop of the angle response

Fig. 9: System response under varying mass ratio λ

By reformulating the system into a series configuration, the pendulum dynamics are stabilized independently via an inner feedback loop, while the cart position is regulated in the outer loop. This structure enables effective separation of dynamics, ensuring faster correction of pendulum deviations and smoother cart positioning. Simulation results show improved transient behavior, reduced overshoot, and robustness against parameter variations and measurement noise. The findings highlight the importance of angle feedback and confirm that properly structured classical control can effectively stabilize and regulate the inverted pendulum system.

Future work will focus on exploring the use of fractional-order PID controllers to achieve a flatter phase response around the crossover frequency. Additional considerations include handling practical constraints such as overshoot limitations due to travel bounds, pendulum angle saturation due to the physical design, actuator nonlinearities arising from friction and pulley dynamics. Finally, the challenges associated with the analog realization of the proposed controller will also be investigated.

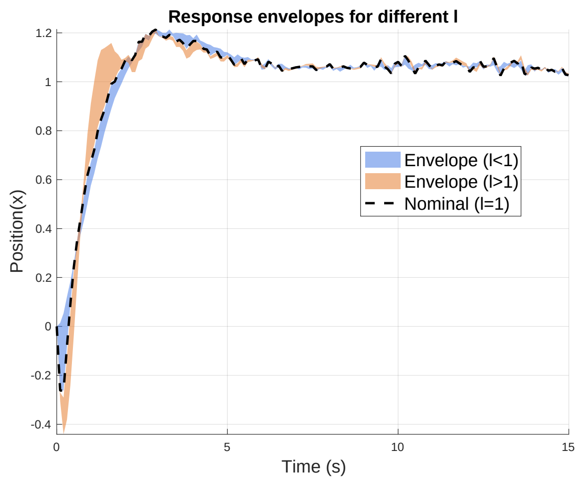

(a) Envelop of the position response

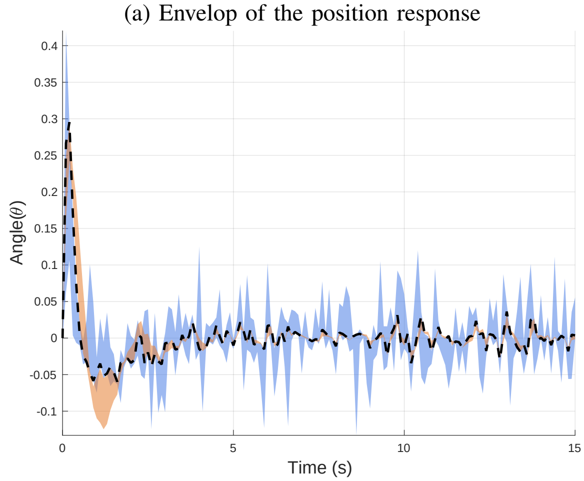

(b) Envelop of the angle response

Fig. 10: System response under varying pendulum length l

A recent lab platform implementation using the PID controller tuning method in this paper is seen from this Youtube short video `https://youtube.com/shorts/Mb7NTytTF-4` while the other controllers tubed by default methods are seen from `https://www.youtube.com/shorts/rZn9-rioyJA` and `https://www.youtube.com/shorts/uTLGBbJM1Z0` We can see that our new controller tuning method is better in control signal smoothness and robustness.

Acknowledgment

The authors were funded in part by the Center for Methane Emission Research and Innovation by the University of California Merced Climate Action Seed Funds grant. (`https://methane.ucmerced.edu`).

Y.Q. Chen would like to acknowledgment the influence of Prof. Kevin L. Moore and Prof. Don Cripps during his time at Utah State University (USU) (2000-2012). The USU Control Systems Teaching Lab has an inverted pendulum on a moving cart platform using a physics lab experimental linear air track, see `https://www.youtube.com/watch?v=y6GFo54DBKo` and `https://youtu.be/TCs4rlPeMes`. It is possible to do an op-amps based purely analog control of the inverted pendulum on a moving cart system. Then, the results of this paper will be useful in tuning the analog PID controllers in dual loop. This idea was discussed by Dr. Don Cripps and Dr. YangQuan Chen in 2007.

References

[1] L. B. Prasad, B. Tyagi, and H. O. Gupta, "Optimal control of nonlinear inverted pendulum dynamical system with disturbance input using PID controller & LQR," in *Proceedings of 2011 IEEE International Conference on Control System, Computing and Engineering*, IEEE, 2011.

[2] E. S. Varghese, A. K. Vincent, and V. Bagyaveereswaran, "Optimal control of inverted pendulum system using PID controller, LQR and MPC," in *Proceedings of IOP Conference Series: Materials Science and Engineering*, IOP Publishing, 2017.

[3] A. I. Roose, S. Yahya, and H. Al-Rizzo, "Fuzzy-logic control of an inverted pendulum on a cart," *Computers & Electrical Engineering*, vol. 61, pp. 31–47, 2017.

[4] L. B. Prasad, B. Tyagi, and H. O. Gupta, "Optimal control of nonlinear inverted pendulum system using PID controller and LQR: performance analysis without and with disturbance input," *International Journal of Automation and Computing*, vol. 11, no. 6, pp. 661–670, 2014.

[5] G. C. Goodwin, S. F. Graebe, and M. E. Salgado, *Control System Design*, vol. 240. Prentice Hall Upper Saddle River, 2001.

[6] D. C. Youla, J. J. Bongiorno Jr, and C. Lu, "Single-loop feedback-stabilization of linear multivariable dynamical plants," *Automatica*, vol. 10, no. 2, pp. 159–173, 1974.

[7] M. M. Seron, J. H. Braslavsky, and G. C. Goodwin, *Fundamental limitations in filtering and control*. Springer Science & Business Media, 2012.

[8] K. J. Åström, "Limitations on control system performance," *European Journal of Control*, vol. 6, no. 1, pp. 2–20, 2000.

[9] S. Skogestad and I. Postlethwaite, *Multivariable feedback control: analysis and design*. John Wiley & Sons, 2005.

[10] J. J. d'Azzo and C. D. Houpis, *Linear control system analysis and design: conventional and modern*. McGraw-Hill Higher Education, 1995.

[11] I. Horowitz and U. Shaked, "Superiority of transfer function over state-variable methods in linear time-invariant feedback system design," *IEEE Transactions on Automatic Control*, vol. 20, no. 1, pp. 84–97, 2003.